

MAGNETIC AND THERMAL ENERGY FLOW DURING DISRUPTIONS IN DIII-D

by

A.W. Hyatt, R.L. Lee, J.W. Cuthbertson, D.A. Humphreys,
A.G. Kellman, C.J. Lasnier, P.L. Taylor,
and the DIII-D Team

MASTER

DISCLAIMER

This report was prepared as an account of work sponsored by an agency of the United States Government. Neither the United States Government nor any agency thereof, nor any of their employees, makes any warranty, express or implied, or assumes any legal liability or responsibility for the accuracy, completeness, or usefulness of any information, apparatus, product, or process disclosed, or represents that its use would not infringe privately owned rights. Reference herein to any specific commercial product, process, or service by trade name, trademark, manufacturer, or otherwise does not necessarily constitute or imply its endorsement, recommendation, or favoring by the United States Government or any agency thereof. The views and opinions of authors expressed herein do not necessarily state or reflect those of the United States Government or any agency thereof.

DISTRIBUTION OF THIS DOCUMENT IS UNLIMITED

JULY 1996 



DISCLAIMER

This report was prepared as an account of work sponsored by an agency of the United States Government. Neither the United States Government nor any agency thereof, nor any of their employees, makes any warranty, express or implied, or assumes any legal liability or responsibility for the accuracy, completeness, or usefulness of any information, apparatus, product, or process disclosed, or represents that its use would not infringe privately owned rights. Reference herein to any specific commercial product, process, or service by trade name, trademark, manufacturer, or otherwise does not necessarily constitute or imply its endorsement, recommendation, or favoring by the United States Government or any agency thereof. The views and opinions of authors expressed herein do not necessarily state or reflect those of the United States Government or any agency thereof.

DISCLAIMER

Portions of this document may be illegible in electronic image products. Images are produced from the best available original document.

MAGNETIC AND THERMAL ENERGY FLOW DURING DISRUPTIONS IN DIII-D

by

A.W. Hyatt, R.L. Lee, J.W. Cuthbertson,[†] D.A. Humphreys,
A.G. Kellman, C.J. Lasnier,[△] P.L. Taylor,
and the DIII-D Team

This is a preprint of a paper to be presented at the Twenty-third European Physical Society Conference on Controlled Fusion and Plasma Physics, June 24–28, 1996, Kiev, Ukraine and to be published in the Proceedings.

[†]University of California, San Diego, California.

[△]Lawrence Livermore National Laboratory,
Livermore, California.

Work supported by
the U.S. Department of Energy
under Contract Nos. DE-AC03-89ER51114,
W-7405-ENG-48, and DE-FG03-95ER54294

GA PROJECT 3466
JULY 1996



MAGNETIC AND THERMAL ENERGY FLOW DURING DISRUPTIONS IN DIII-D*

A.W. Hyatt, R.L. Lee, J.W. Cuthbertson,[†] D.A. Humphreys, A.G. Kellman, C.J. Lasnier,^Δ
P.L. Taylor, and the DIII-D Team

General Atomics, P.O. Box 85608, San Diego, California 92186-9784 USA

We present results from disruption experiments where we measure magnetic energy flow across a closed surface surrounding the plasma using a Poynting flux analysis to measure the electromagnetic power, bolometers to measure radiation power and IR scanners to measure radiation and particle heat conduction to the divertor. The initial and final stored energies within the volume are found using the full equilibrium reconstruction code EFIT. From this analysis we calculate an energy balance and find that we can account for all energy deposited on the first wall and the divertor to within about 10%.

INTRODUCTION

A disruption is an abrupt termination of a tokamak discharge, usually caused by a loss of MHD stability, in which the magnetic and thermal energy stored in the tokamak is rapidly lost. Disruptions in an ITER-scale fusion device are projected to distribute in excess of 1 GJ of thermal and 1 GJ of magnetic energies to in-vessel tokamak components on a time scale of milliseconds. The energy flow magnitude, the spatial distribution, the time scale and the loss mechanism taken to the various in-vessel components are critical issues for any large tokamak and resolution of these issues will have a significant impact on the engineering costs and the lifetime and reliability of the components.

We have begun dedicated disruption experiments on the DIII-D tokamak¹ to address these issues. DIII-D has a large complement of disruption relevant diagnostics, including fast core and divertor Thomson scattering, toroidal and poloidal arrays of halo current monitors, fast ECE, fast Xuv spectrometry, several IR scanners viewing different internal wall locations, and multichannel bolometry that covers the inner chamber. The DIII-D tokamak has a robust internal mechanical structure to withstand a disruption's electromechanical forces. Conditioning of the vessel and carbon first wall, including baking to 350°C, boronization, and inter-shot helium glow cleaning provides immediate recovery from high power disruptions.

This paper describes an effort to address the disruption energy flow/energy balance issues by measuring the magnetic, radiative and conductive power fluxes. We use the MHD equilibrium reconstruction code EFIT² coupled with a Poynting flux analysis³ at a surface nested just within the conducting vacuum wall, multichannel bolometry, and two toroidally separated infrared (IR) scanners with full radial view of the divertor floor.

ENERGY FLOW ANALYSIS METHOD

In the paper we are concerned with energy flows and energy balance within the first wall defined surface. Of particular interest is the flow of energy in or out of the surface, specifically through radiation, conduction and electromagnetic energy flow. We begin by applying conservation of energy,

$$\frac{\partial W_{TOT}}{\partial t} + \int_{\text{surface}} S_{TOT} \cdot \hat{n} dA = 0 \quad , \quad (1)$$

where $W_{TOT} = W_M + W_{TH}$, $W_M = \int dV (\mathbf{B} \cdot \mathbf{H} + \mathbf{E} \cdot \mathbf{D})$, W_{TH} is the plasma thermal energy, $W_M = W_{MT} + W_{MP}$ and W_{MP} , W_{MT} are the poloidal and toroidal magnetic field energies respectively. The contribution of the $\mathbf{E} \cdot \mathbf{D}$ term is small and can be neglected. $S_{TOT} = S_{AUX} + S_{EM} + S_{COND} + S_{RAD}$ where S_{AUX} is the input auxiliary heating flux, $S_{EM} = (\mathbf{E} \times \mathbf{H})$ is the Poynting flux of electromagnetic energy across the surface, S_{COND} is the thermal energy conducted across the surface, and S_{RAD} is the

*Work supported by the U.S. Department of Energy under Contract No.s DE-AC03-89ER51114 and W-7405-ENG-48 and Grant No. DE-FG03-95ER-54294.

[†]University of California, San Diego, California.

^ΔLawrence Livermore National Laboratory, Livermore, California

energy radiated across the surface. Power balance can be written in terms of two coupled equations:

$$dW_{TH}/dt = P_{OHM} - P_{AUX} - P_{RAD} - P_{COND} \quad (2)$$

and

$$dW_M/dt = -P_{EM} - P_{OHM} \quad (3)$$

Here P_{OHM} , P_{AUX} , P_{RAD} , P_{COND} and P_{EM} are the surface integrals of S_{AUX} , S_{RAD} , S_{COND} and S_{EM} , and $P_{OHM} = \int \mathbf{J} \cdot \mathbf{E} \, dV$ is the conversion of electromagnetic energy to thermal energy.

For DIII-D we choose a closed toroidally symmetric surface just inside the vacuum vessel surface, but outside the first wall, as shown in Fig. 1. This surface passes through a set of 31 magnetic probes so that H_p is measured directly on the surface. The Poynting flux in an axisymmetric system consists of two components: $(\mathbf{E} \times \mathbf{H}) \cdot \hat{n} \, dA = (E_p H_\phi - E_\phi H_p) \, dA$, where \hat{n} points outwards from surface A, ϕ is in the toroidal direction, and $\mathbf{p} = \phi \times \hat{n}$. Then $P_{EM} = P_{EMT} + P_{EMP}$, where P_{EMT} is due to $E_p H_\phi$ and P_{EMP} is due to $E_\phi H_p$. A full time-dependent reconstruction with the code EFIT provides $R E_\phi = -2\pi \partial \phi / \partial t$ on the surface, where R is the major radius, and hence one component of the Poynting flux at the surface is unambiguously measured. EFIT also calculates the time dependent W_M and W_{TH} . The local value of the toroidal electric field is known, but only the average poloidal electric field. The average poloidal electric field $\langle E_p \rangle = L^{-1} \partial \Phi / \partial t$, where L is the poloidal length of the surface and Φ is the enclosed toroidal flux. $\partial \Phi / \partial t$ is approximately measured by a diamagnetic flux loop just outside the vessel wall.

It can be shown that in the tokamak if the change in toroidal field is small, i.e. $B_T = B_{T0}(1+\delta)$ with $\delta \ll 1$, then to lowest order $dW_{MT}/dt + P_{EMT} \approx 0$. Then the change in toroidal field energy, ΔW_{MT} , passes through the surface as $\int dt P_{EMT}$. This near equality is confirmed by specific example in the next section.

Using the full equilibrium reconstruction from EFIT gives an accurate representation of the time dependent Poynting flux. However, robust equilibria are not yet available throughout the entire disruption process; progress is still being made on improving the robustness of solutions during disruptions. We can still estimate the total amount of electromagnetic energy crossing the surface. We note, following Hosogane⁴ that the poloidal field coil cage defines a highly conducting boundary; see Fig. 1. During the time of the disruption, the electromagnetic energy flux crossing this boundary is very small, so that the electromagnetic energy flux across the surface just inside the vacuum vessel is approximately equal to the net change in electromagnetic energy in the annulus between the poloidal coils and surface A. We term this assumption the "coil cage assumption" and use it in the following energy flow calculations to carry the analysis past the point where EFIT does not converge well.

P_{COND} is measured using Inframetrics 525 IR scanners at 8 kHz.⁵ The scanners view a radial chord spanning the lower divertor floor at two toroidal locations 105 degrees apart. Each scanner has about 5 ms dead time every 16.7 ms and cannot be externally synchronized, so any given disruption may have incomplete coverage. A one dimensional model is used to convert measured temperatures to heat flux.⁶ Where there is toroidal asymmetry in the calculated heat flux a simple average is used. Toroidal asymmetries of deposited energies ($Max/Average$) of up to 1.6 have been observed.

P_{RAD} is measured using two poloidally separated 24 channel metal foil resistor bolometer arrays.⁷ The total power is calculated using the sum of all channels' line averaged power and by geometrically constraining the radiating volume with EFIT reconstructed boundaries. The last reconstructed EFIT boundary is assumed for times after successful EFIT reconstruction stops. This assumption should have only a small effect on the total radiated energy.

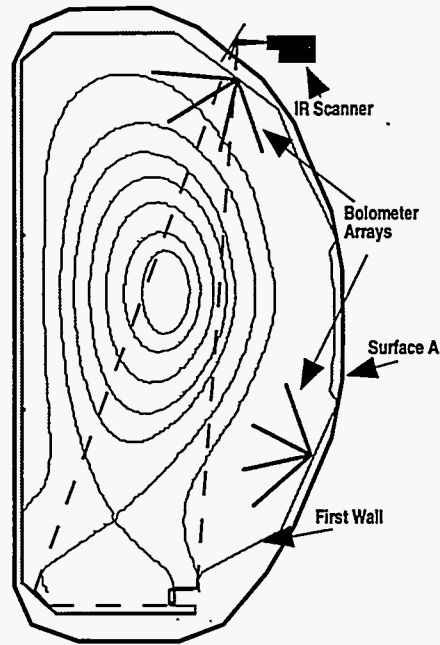


Fig. 1 A cross sectional view of DIII-D showing the poloidal locations and tokamak views of the IR scanners and bolometer arrays. The outermost line denotes Surface A. The line labeled First Wall denotes the plasma facing carbon armor surface. Not shown is the vacuum vessel inner wall which lies just outside Surface A.

With use of the Poynting flux, all of the components of the energy flux in Eqs. (2) and (3) except P_{OHM} and P_{AUX} are determined. P_{OHM} need not be explicitly determined for an accurate energy flux accounting, since it simply transfers energy from the magnetic to the thermal within the surface. Only neutral beam heated discharges are considered here, and P_{AUX} is determined from the measured accelerating voltages and neutral currents.

EXPERIMENTAL RESULTS

Three types of disruptions are analyzed: #84356, a high beta disruption precipitated by exceeding the expected MHD high beta stability limit; shot #81168, a disruption precipitated by an argon gas puff induced radiative collapse, and #88824, a Vertical Displacement Event (VDE), precipitated by disabling the vertical feedback controls. The evolution of 84356 is shown in Fig. 2. For reasons discussed above we omit W_{MT} and P_{EMT} in the following analysis. We choose t_0 at 2200 ms, and t_{end} at 2240 ms, when the plasma current has vanished. At t_0 EFIT calculates a total energy $W(t_0) = W_{TH}(t_0) + W_{MP}(t_0) = 1.01 \text{ MJ} + 1.33 \text{ MJ} = 2.34 \text{ MJ}$. From a central soft x-ray signal we see that there is a large initial dump of thermal energy at 2212 ms which is followed by the thermal quench (TQ) at 2222 ms. The EFIT reconstruction at $t_{TQ} = 2223 \text{ ms}$ shows that W_{TH} has dropped to nearly zero. The energy remaining is then measured to be $W(t_{TQ}) = W(t_0) - \int (P_{AUX} + P_{EMP} + P_{COND} + P_{RAD}) dt = 1.41 \text{ MJ}$. Over this interval $\int dt P_{AUX}$ has input 0.40 MJ of thermal energy, and $\int dt P_{EMP}$ has input 0.06 MJ of magnetic energy. The bolometers measure $\int dt P_{RAD} = 0.70 \text{ MJ}$ radiatively flowing out of the volume, and the IR scanners measure $\int dt P_{COND} = 0.69 \text{ MJ}$ conducted out calculated from the 0.83 MJ thermal flux measured by the IR scanners minus the 0.14 MJ of energy radiated to the divertor measured by bolometry tomography. At t_{TQ} EFIT calculates $W_{TH} = 0$ and $W_{MP} = 1.44 \text{ MJ}$. If we define an energy balance $EB = \int (P_{AUX} + P_{EMP} + P_{COND} + P_{RAD}) dt / [W(t_0) - W(t_{end})]$ and express EB as a percentage, then at the thermal quench $EB = 103\%$, i.e. the net energy flow is accounted for to within 3%. This measure of energy balance is attractive in that all the measured flows are in the numerator, and only end point EFIT reconstructions are in the denominator. Measurement errors are estimated to be $\pm 10\%$ for the bolometers and the IR scanners, and $\pm 5\%$ for EFIT. We employ the coil cage assumption to carry the analysis to t_{end} . This implies a total of about 0.47 MJ of magnetic energy input during the disruption. Then the measured net energy flow leaves 0.26 MJ in the volume at t_{end} while EFIT calculates 0.17 MJ of vacuum magnetic energy for an overall $EB = 96\%$.

From P_{EMT} determined experimentally from diamagnetic loop measurements, we find $\int dt P_{EMT} = 0.3 \text{ MJ}$ flowing out of the vessel over the span of the disruption. The change in the toroidal magnetic energy calculated by EFIT, $\Delta W_{MT} = -0.3 \text{ MJ}$, as expected. So to within the accuracy of the measurement all of the diamagnetic energy within the surface flows electromagnetically through the surface and is not converted to thermal energy which might appear on the first wall.

Analyses for all three cases are summarized in Table 1. In the second row we see that the net energy flow is accounted for to within 10% or better for the first two cases; for the VDE the overall energy flow is 22% too large. We believe the over counting is due to the relatively low level of pre-disruption energy. The third row displays the pre-disruption energies and the measured total magnetic and thermal energy inputs. In the cases shown there is a net flow of electromagnetic energy, ΔW_{EMP} , into the vessel

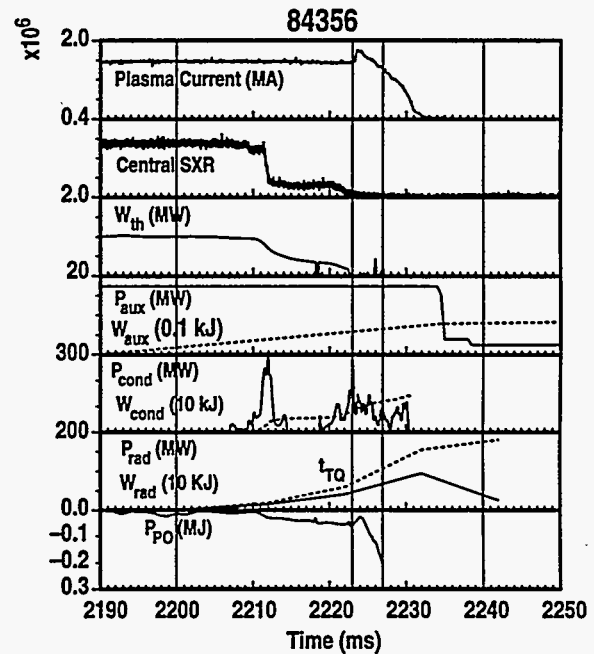


Fig. 2. Time history of the disruption. The central soft xray signal shows the initial thermal collapse followed by the thermal quench at 2223 ms. The vertical lines are t_0 , t_{TQ} , t_{EFIT} , t_{end} from left to right. P_{AUX} , P_{COND} and P_{RAD} are shown as solid lines with the integrated power as dashed. W_{EMP} is the net energy flow out of the surface due to P_{EMP} . Note W_{EMP} is negative; magnetic energy flows into the plasma chamber during the disruption.

TABLE 1

Discharge Type Current, Field	81168 Radiative Collapse 1.5 MA, 2.1 T	84356 High Beta 1.5 MA, 1.2 T	88824 VDE 1.0 MA, 1.0 T
EB at TQ	110%	103%	102%
EB overall	111%	96%	122%
$W_{TH}(t_0)$	1.17	1.01	0.53
$W_{MP}(t_0)$	1.53	1.33	0.64
ΔW_{EMP}	0.50	0.47	0.19
ΔW_{AUX}	0.41	0.54	0.11
$W_{COND}/W(t_0)$	0.67/2.70 = 25%	1.16/2.34 = 50%	0.68/1.17 = 58%
$W_{RAD}/W(t_0)$	2.88/2.70 = 107%	1.75/2.34 = 75%	0.90/1.17 = 77%
$W_{FW}(t_{TQ})/W(t_0)$	2.18/2.70 = 81%	1.39/2.34 = 59%	0.71/1.17 = 61%
$W_{FW}(t_{end})/W(t_0)$	3.55/2.70 = 132%	2.91/2.34 = 124%	1.58/1.17 = 135%

$W(t_0) = W_{TH}(t_0) + W_{MP}(t_0)$, the initial stored energy at t_0 , in MJ

$W_{FW}(t)$ = energy deposited on inner walls & divertor, in MJ, at time t

W_{COND} = total energy conducted to divertor, in MJ

W_{RAD} = total energy radiated to first wall, in MJ

ΔW_{EMP} = total magnetic energy input from P_{EMP} , in MJ

ΔW_{AUX} = total thermal energy input from P_{AUX} , in MJ

during the disruption which is approximately 30% of the pre-disruption magnetic energy stored within the vacuum vessel. The fourth row displays the measured conducted and radiated energy flows normalized to $W(t_0)$, the total pre-disruption energy. Radiation dominates, and for the radiative collapse case it strongly dominates; the extra radiation comes at the expense of conducted power. The radiative collapse case conducts about half of its pre-disruption thermal energy to the divertor, while the other cases conduct more than 100%. The fifth row displays the total net energy that flows to the first wall, W_{FW} , similarly normalized, at t_{TQ} and t_{end} . We see that in all cases ~130% of W_0 , the total pre-disruption energy, eventually flows to the walls. This is due in part to ΔW_{EMP} , the total electromagnetic energy inflow during the disruption, and to ΔW_{AUX} , the total thermal energy inflow from P_{AUX} . Presumably ΔW_{AUX} can be significantly decreased if auxiliary heating is terminated earlier in the disruption, but ΔW_{EMP} is not likely to decrease.

DISCUSSION

The Poynting flux analysis described here provides a precise method to measure magnetic energy flow into and out of the vacuum vessel volume. It may also prove beneficial for similar energy flow measurements to the vacuum vessel itself, and to structure outside the vacuum vessel. The energy balance based upon it give a total accounting of energy flows to roughly 10%. Analysis indicates that net electromagnetic energy flows into the plasma during disruptions where it is converted to thermal energy and deposited on the first wall. In DIII-D the assumption that the relevant volume for calculating the stored magnetic energy is defined by the poloidal field coils gives a good overall energy balance, and this is likely more or less true for any tokamak with a resistive vessel depending on the details of the coil cage. Projections which assume that only the stored magnetic energy associated with the plasma internal inductance, I_p , will be deposited in a disruption will be too low; in DIII-D by a factor of 2. The data indicates that unless mitigation efforts are employed over 100% of the pre-disruption thermal energy will be conducted to the divertor. Finally, the data indicates that the plasma diamagnetic energy is not converted to heat which may be conducted or radiated to the first wall.

¹Taylor, P.L., et al., Phys. Rev. Lett. **76**, (1996) 916; Evans, T.E., et al., "Non-Axsymmetric Halo Currents With and Without "Killer" Pellets During Disruptive Instabilities in DIII-D," to be published in J Nucl. Mater.

²L.L. Lao, et al., Nucl. Fusion **25**, (1985) 1611.

³Ejima, et al., Nucl. Fusion **22**, (1982) 1313.

⁴Hosogane, JAERI-M 90-066.

⁵Lee, R.L., et al., "Thermal Deposition Analysis During Disruptions on DIII-D Using Infrared Scanners," Proc. 16th Symp. on Fusion Engineering,, (Institute of Electrical and Electronics Engineers, Inc. Piscataway, New Jersey) to be published.

⁶Hill, D.N., Ellis, R., Fergusen, S.W., Perkins, D.E., Rev. Sci. Instrum. **59**, (1988) 1878.

⁷Leonard, A.W., et al., Rev. Sci. Instrum. **66**, (1995) 1201.